Site-Directed Mutagenesis Probing the Catalytic Role of Arginines 165 and 166 of Human Cytomegalovirus Protease

Po-Huang Liang, Kimberly A. Brun,‡ John A. Feild,‡ Kevin O'Donnell, Michael L. Doyle, Susan M. Green, Audrey E. Baker, Michael N. Blackburn, and Sherin S. Abdel-Meguid*

Department of Macromolecular Sciences and Molecular Genetics, SmithKline Beecham Pharmaceuticals, 709 Swedeland Road, King of Prussia, Pennsylvania 19406

Received October 21, 1997; Revised Manuscript Received March 6, 1998

ABSTRACT: Human cytomegalovirus (CMV) is a member of the *Herpesviridae* family of viruses that also includes herpes simplex viruses (HSV-1 and HSV-2), varicella-zoster virus (VZV), human herpes virus-6, 7, and 8 (HHV-6, HHV-7, and HHV-8), and Epstein−Barr virus (EBV). Each member of this family encodes a serine protease that is a potential target for antiviral therapeutic intervention. We recently reported the crystal structure of CMV proteases [Qiu, X., Culp, J. S., DiLella, A. G., Hellmig, B., Hoog, S. S., Janson, C. A., Smith, W. W., and Abdel-Meguid, S. S. (1996) *Nature 383*, 275−279] and proposed that the highly conserved Arg165 and Arg166 residues are involved in stabilizing the oxyanion intermediate in human herpes protease catalyzed reactions through the backbone NH and side chain, respectively. In the current study, site-directed mutagenesis was carried out to probe the catalytic function of these two amino acid residues. Substitution of Arg166 with an alanine has led to ablation of enzymatic activity without detectable change in CMV protease conformation, supporting suggestions from the crystal structure that Arg166 side chain plays a major role in catalysis. The wild-type has a $K_m = 138 \pm 17$ μM and $k_{cat} = 19.9 \pm 1.1$ min^{-1}, while R166A has only residual activity, with a $k_{cat} = 0.012 \pm 0.001$ min^{-1} and an unaltered $K_m = 145 \pm 18$ μM. In the crystal structure, the side chain of Arg166 was shown previously to hold a water molecule that can act as a hydrogen-bond donor to the oxyanion and was thus proposed to stabilize the oxyanion intermediate. However, kinetic characterization of the mutant R165A only reveals a 2.7-fold lower activity than wild-type, with a $K_m = 166 \pm 19$ μM and a $k_{cat} = 7.4 \pm 0.4$ min^{-1}. These results confirm that Arg165 side chain is not involved in the stabilization of the oxyanion. It is likely that Arg165 only utilizes the backbone NH for catalysis as suggested by the crystal structure.

The herpes virus family is divided into three subfamilies designated α, β and γ. The α subfamily includes herpes simplex viruses 1 and 2 (HSV-1 and HSV-2)[1] and varicella-zoster virus (VZV); β includes cytomegalovirus (CMV) and human herpes viruses 6 and 7 (HHV-6 and HHV-7); and γ includes Epstein−Barr virus (EBV) and human herpes virus 8 (HHV-8). Human CMV is a ubiquitous opportunistic pathogen that can result in life threatening infections in congenitally infected infants, immunocompromised individuals and immunosuppressed transplant patients. It encodes a 708 residue serine protease essential for its replication (*1, 2*).[2] The protease undergoes autoproteolytic cleavage at two sites. The first site near the carboxy-terminus is known as the maturation (M) site, while the second (R-site) is responsible for the release of a 256 amino-terminal domain having full catalytic activity (*1*). The latter can be further cleaved at an internal site [between Ala143 and Ala144 (*3*)] to form an active heterodimeric protease, but this internal cleavage can be avoided by mutation, and the mutation did not alter enzyme kinetic properties (*4*). In the present studies, we utilize a A143V mutant form of CMV protease to stabilize the protease against autofragmentation.

Although CMV protease is a serine protease (*5*), it shares no sequence homology or structural analogy with classical serine proteases (*3, 6*). Furthermore, unlike classical serine proteases in which the catalytic mechanism involves an active-site triad composed of a serine, a histidine, and an aspartic acid, CMV protease utilizes a serine and two histidines to catalyze its reaction (*7*−*10*). These and other unique properties of CMV protease suggest that it belongs to a new subclass of serine protease family.

The crystal structures of CMV, VZV, HSV-1, and HSV-2 proteases have been reported (*7*−*12*). Overlays of the catalytic triad of any of these structures with that of trypsin suggested that Arg165 and Arg166 (CMV protease number-

* To whom correspondence should be addressed.

‡ Molecular Genetics.

[1] Abbreviations: CMV, cytomegalovirus; VZV, varicella-zoster virus; HSV, herpes simplex virus; HHV, human herpesvirus; EBV, Epstein−Barr virus; kDa, kilodaltons; Dabsyl, 4-*N*, *N*-dimethylaminoazobenzene-4′-sulfonyl; Dansyl II, 2-dimethylaminonaphthalene-5-sulfonyl; Tris, tris(hydroxymethyl)aminomethane; Hepes, 4-(2-hydroxyethyl)-1-piperazineethanesulfonic acid); DTT, dithiothreitol; EDTA, ethylenediaminetetraacetic acid; PEG, poly(ethylene glycol); SDS−PAGE, sodium dodecyl sulfate−polyacrylamide gel electrophoresis; MALDI, matrix-assisted laser desorption and ionization; Ni^{2+}NTA, nickel nitrilotriacetic acid; K_m, Michaelis constant; $k_{cat} = V_{max}/[E]_t$ in which V_{max} is maximum velocity and $[E]_t$ is total enzyme concentration; K_d^{app}, apparent dissociation constant.

[2] The protease has only been shown to be essential in HSV-1 [Gao et al. (1994) *J. Virol. 68*, 3702−3712], and is assumed to be essential in other herpes viruses based on homology.

S0006-2960(97)02607-X CCC: $15.00
Published on Web 04/09/1998

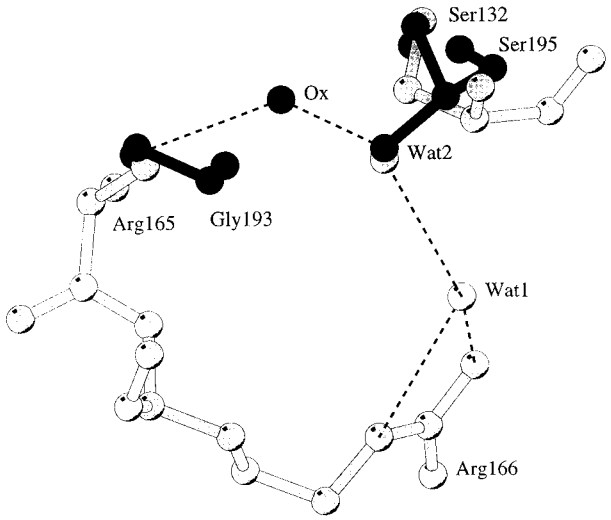

FIGURE 1: Overlay of the CMV protease active site with that of the classical serine protease trypsin, focusing on the amino acids responsible for oxyanion stabilization.[3] The stereoview was drawn in the ball-and-stick representation with the computer program MOLSCRIPT. The CMV protease is shown in light and trypsin is shown in dark. Ox and Wat represent oxyanion and water, respectively. Hydrogen bonds are represented by broken lines.

ing) are involved in stabilization of the oxyanion intermediate. Such overlays resulted in superposition of Arg165 backbone atoms with those of Gly193 of trypsin (Figure 1). The latter is known to stabilize the oxyanion intermediate through a hydrogen bond with its backbone NH. Ser195 of trypsin is also known to stabilize the enzyme active site oxyanion intermediate through a hydrogen bond with its backbone NH. The equivalent residue in the herpes proteases is absent. Instead, a water molecule held by the side chain of Arg166 in the viral proteases was proposed to form a hydrogen bond with the oxyanion (*7, 9*). However, Tong et al. (*8*) have proposed that the oxyanion hole in CMV protease is formed by the main-chain amido groups of residues 165 and 166 and a water molecule is associated with two groups in the crystal structure. On the other hand, Chen et al. (*10*) have suggested that either or both Arg165 and Arg166 side chains could hydrogen bond directly to the oxyanion. To test the role of Arg165 and Arg166 side chains in the stabilization of the oxyanion intermediate, we have mutated each of these residues and characterized these mutant enzymes.

Biophysical and biochemical studies have shown that human CMV protease is active as a homodimer (*13*−*15*). Here, we report characterization of the Michaelis−Menten steady-state K_m and k_{cat} parameters of the CMV protease homodimer and its two suspected oxyanion pocket mutants. The data implicate the role of Arg165 and Arg166 in the stabilization of the oxyanion intermediate.

EXPERIMENTAL PROCEDURES

Construction of Wild-Type and Mutants. The CMV protease gene that includes the amino-terminal 256 amino acids of UL80 was synthesized using preferred *Escherichia coli* codons. Previous kinetic studies of human CMV protease have utilized forms of the enzyme in which either Ala143 or Ala144 was mutated to stabilize the protease against internal cleavage at this site (*12, 13*). Similarly, all three of our constructs include an A143V mutation for stabilization. For simplicity, the singly modified A143V mutant will be referred to as wild-type, while the doubly modified A143V/R165A or A143V/R166A mutants will be referred to as R165A and R166A, respectively. Another modification located after the release site (R-site) is the addition of a 12 amino acid extension (VSPEAAADIKAA) followed by a hexahistidine tag to allow for purification by immobilized metal affinity chromatography. The amino acid sequence of the 12 residue extension is that (with C changed to A in the seventh amino acid from left in the sequence) of the authentic sequence of UL80 following the R-site, and thus allows for self-processing at R-site after purification.

The synthetic CMV protease gene was subcloned between the *Nde*I and *Bam*HI sites of the pET22b *E. coli* expression vector (Novagen, Madison, WI). Site-directed mutagenesis was performed according to the manufacturer's instructions using the QuikChange Site-Directed Mutagenesis Kit (Stratagene, La Jolla, CA). The only modification to the protocol was the ethanol precipitation of the mutagenesis primers rather than gel purification. The following oligonucleotides were used as primers for mutagenesis: R165A, 5′-GCT-CTG-TGC-TCC-GTT-GGT-gcT-CGC−CGC-GGT-ACC−CTG-GC-3′ and 5′-GC−CAG-GGT-ACC-GCG-GCG-Agc-ACC-AAC-GGA-GCA-CAG-AGC-3′, R166A, 5′-GCT-CTG-TGC-TCC-GTT-GGT-CGT-gcT-CGT-GGT-ACC−CTG-GC-3′ and 5′-GC−CAG-GGT-ACC-ACG-Agc-ACG-ACC-AAC-GGA-GCA-CAG-AGC-3′.

Four colonies each were picked from the R165A and the R166A mutagenesis transformation plates, and plasmid DNA was isolated using the Qiagen mini prep kit (Qiagen, Santa Clarita, CA). Mutations were confirmed by dye terminator cycle sequencing (Perkin-Elmer, Foster City, CA) using an Applied Biosystems Model 373 automated DNA sequencer. A single mutant clone was selected and transformed into LW29(DE3) competent cells for *E. coli* expression. LW29 (DE3) competent cells are a derivative of W3110lacIq cells, a K12 strain (*16*), that have been lysogenized with λ (DE3).

Expression of Mutants. Two 1 L flasks containing 200 mL of LB medium supplemented with 50 μg/mL of ampicillin were inoculated with the pET22bCMV mutant plasmids and grown in a 37 °C shaker incubator overnight at 245 rpm. The next morning, 30 mL of the overnight cultures was added to 500 mL of LB medium containing 50 μg/mL ampicillin and grown at 37 °C. When the A_{650} of the cultures reached 0.75−0.8, 500 mL of 4 °C LB medium was added to the cultures and grown at 25 °C for an additional 15 min. Expression of the mutant proteins was induced by adding isopropyl β-D-thiogalactopyranoside to a final concentration of 1 mM. Growth continued at 25 °C for 1 h. A 0.5 mL sample was taken before induction and 1 h after induction. The samples were spun at 12500*g*, and the cell pellets were resuspended in 2× sample buffer (2% SDS, 10% glycerol, 8 mM Tris-CL pH 6.8, 0.008% bromophenol blue, and 5% 2-mercaptoethanol). The remainder of the cell culture was centrifuged at 4200*g* for 30 min, and the cell pellets were frozen at −20 °C prior to purification.

Western Blot Analysis of Mutant Proteins. To check for induction of mutant proteins, lysates of cells harboring the

[3] In the crystal structure of CMV protease (*7*), we observed one water molecule in the active site. However, modeling suggests that two water molecules are in the active site to form hydrogen-bonding network.

mutant plasmid were subjected to electrophoresis on a 15% SDS−PAGE gel under reducing conditions according to Laemmli (*17*). Using the method of Towbin et al. (*18*), protein samples were transferred to 0.2 μm nitrocellulose paper. The primary antibody was a rabbit polyclonal antibody recognizing the CMV protease domain, the secondary antibody was a horseradish peroxidase conjugated sheep IgG fraction to rabbit IgG (Cappel, West Chester, PA). ECL (Amersham, Arlington Heights, IL) was used to detect mutant protein expression.

Protein Purification. As discussed above, the catalytically active domain of human CMV protease is expressed with an autoprocessing linker region on the carboxy-terminus followed by a hexahistidine tag. The tag was used to facilitate purification of protein by Ni^{2+}NTA affinity column chromatography. All purification steps were carried out at 4 °C. For cell lysis, the thawed cells were suspended in buffer (50 mM Tris and 300 mM NaCl, pH 8.0) at 10 mL/g of cell using a Tekmar Tissumizer. The cells were lysed with a single pass through the EmulsiFlex C-30 at 12 000 psi (Avestin, Inc., Canada). The lysate was centrifuged for 1 h at 30000*g*, and the pellet was discarded. The supernatant was mixed with 10 mL of Ni^{2+}NTA resin (Qiagen Co.) and incubated at 4 °C for 1 h. The mixture was then centrifuged at 2560*g* for 10 min at 4 °C. Most of the supernatant was removed with a pipet, and the residual resin with bound proteins was packed into a Pharmacia XK column (1.6 × 5 cm). The column was washed with buffer (50 mM Tris and 300 mM NaCl, pH 8.0) at a flow rate of 40 cm/h and then with the same buffer containing 50 mM imidazole (Calbiochem Co.) until a stable baseline was obtained. The column was eluted with buffer containing 250 mM imidazole at the same flow rate. The eluted sample was concentrated and exchanged into buffer containing 25 mM Hepes, pH 8.0, 50 mM NaCl, 10 mM DTT, 2 mM EDTA, and 10% glycerol in a 50 mL Amicon stirred cell with a YM10 membrane at 65 psi and 4 °C. The protease was allowed to autoprocess at 4 °C overnight (for wild-type) or for several days until completely processed (for R165A mutant). The sample after autoprocessing was concentrated and filtered through a Millipore Millex HV_{13} 0.45 μ syringe filter. The filtered sample was loaded onto a 120 mL Pharmacia Superdex 75 column (1.6 × 60 cm) and eluted with 25 mM Hepes, 2 mM DTT, and 1 mM EDTA, pH 8.0 at 30 cm/h. The eluted protease was concentrated and microcentrifuged at 17000*g* for 10 min at 4 °C, and the supernatant was filtered through 0.22 μ Millipore Millex GV syringe filter. Glycerol was added to 50% (V/V). The autoprocessing was confirmed by protein SDS−PAGE and MALDI mass spectrometry. The protein was stored with 50% glycerol at −20 °C. After purification, both wild-type CMV protease and the R165A mutant were His-tag free. The R166A mutant was almost inactive and failed to autoprocess its His-tag.

Removal of His-Tag from R166A Mutant. To remove the His-tag from purified R166A mutant, an active wild-type CMV protease with a noncleavable N-terminus His-tag was constructed and purified using the same procedure as mentioned above. The His-tag on R166A mutant was then removed by incubating C-terminus His-tagged R166A with the noncleavable His-tagged CMV protease in a $^1/_{20}$ molar ratio at 4 °C overnight. Following processing, the solution was concentrated and the buffer exchanged into 50 mM Tris, 300 mM NaCl, and pH 8.0. R166A was purified from the N-terminus His-tagged CMV protease by passage over a 2 mL Ni^{2+}NTA column. R166A was in the flow through. It was then concentrated as above, and the buffer was exchanged to 25 mM Hepes, pH 8.0, 2 mM DTT, and 1 mM EDTA. The sample was centrifuged in a microfuge to sediment any particulate matter and was loaded in two batches onto a Superdex 75 column (1.6 × 30 cm) and eluted at 1 mL/min. The fractions containing R166A were pooled, concentrated, and made 50% in glycerol. As above, the processing was confirmed by SDS−PAGE and MALDI mass spectrometry.

Kinetic Constant (K_m and k_{cat}) and Apparent Dissociation Constants (K_d^{app}) Measurements. The kinetic studies were carried out in 50 mM Hepes buffer (pH 7.5) containing 150 mM NaCl, 1 mM EDTA, 1 mM DTT, 0.01% (W/V) PEG 3400, and 30% (W/V) sucrose (Ultrapure grade, Sigma Co.) at 25 °C. All enzyme solutions were prepared in siliconized sepratubes (Integrated Separation Systems). A fluorophore-labeled peptide (Dabsyl-DGVVNASSRLADK (Dansyl II)-OH was used as a substrate. Enhanced fluorescence of the cleaved peptide was monitored at 496 nm with an SLM 8000 Spectrofluorometer with excitation at 365 nm. Reactions were terminated by taking an aliquot of reaction mixture and diluting it into 9 mM Zn^{2+} solution [a known inhibitor of CMV protease with a K_i near 1 μM (*19*)] to a final concentration of 5 μM substrate. At 5 μM substrate, the inner filter effect is negligible. At timed intervals, samples were vortexed into Zn^{2+} and the amount of product was determined from the enhanced fluorescence. The slope of the fluorescence change over three time points was used to calculate the reaction rate. The maximum enzyme concentrations used for K_m and k_{cat} measurements were 0.05, 0.15, and 10 mM for wild-type, R165A, and R166A, respectively. The initial rate was measured with less than 10% substrate depletion. Data of initial rates vs substrate concentrations were analyzed by nonlinear regression of the Michaelis−Menten equation using the KaleidaGraph computer program (Abelbeck software) to obtain K_m and V_{max}. The k_{cat} value for the dimeric protease was calculated from V_{max}, total enzyme concentration, and the apparent monomer−dimer dissociation constants K_d^{app}.

Enzyme concentration ranges of 0.01−0.2 μM for wild-type protease, 0.02−0.2 μM for the R165A mutant, and 2−20 μM for R166A were used in measurements of the apparent monomer−dimer dissociation constant K_d^{app}. The equilibrium monomer−dimer K_d of wild-type CMV protease was measured using 0.01−1 μM protease which was allowed to equilibrate at 25 °C for 18 h. The reaction was initiated by adding substrate (final concentration of substrate was 30 μM for wild-type and R165A and 50 μM for R166A) to 50 mM Hepes, 150 mM NaCl, 1 mM EDTA, 1 mM DTT, 0.01% PEG 3400, and 30% sucrose, pH 7.5, 25 °C, containing various concentrations of enzyme. For wild-type and R165A, portions of the reaction mixture were terminated at various times by mixing with 9 mM Zn^{2+}. For R166A, due to its extremely low activity, a fluorescence plate reader CytoFluor (PerSeptive Biosystems, Framingham, MA) was used to measure the relative activities of 2−20 μM enzyme. Due to inner filter effect of 30 μM substrate, the reaction rate of different concentration of R166A was determined by

comparing with known activity (measured as mentioned above) of wild-type CMV protease under the same assay condition. The monomer−dimer dissociation constants were obtained by fitting reaction rates versus enzyme concentration to the following equations (*14*).

$$K_d = [M]^2/[D] \quad (1)$$

$$[D] = 1/8(K_d + 4[E]_t - \sqrt{K_d^2 + 8K_d[E]_t}) \quad (2)$$

$$v = As[1/8(K_d + 4[E]_t - \sqrt{K_d^2 + 8K_d[E]_t})] \quad (3)$$

In these equations, [D] is dimer concentration, [M] is monomer concentration, the total enzyme concentration $[E]_t = [M] + 2[D]$, v is the observed reaction rate, and As is the activity of dimer. In our analyses and other reports *(13, 14)*, the activity of the monomer was unmeasureably low (≤1% of the dimer activity) and is thus assumed to be inactive in eq 3.

Circular Dichroism Studies. Circular dichroism measurements were made on a Jasco J-710 spectropolarimeter in a 0.1 cm water-jacketed cuvette. Solution conditions were 0.25 mg/mL protease, pH 7.4, 5 mM $NaHPO_4$, 150 mM NaCl, 0.5 mM EDTA, 1 mM DTT, and 10% glycerol. Spectra reported are the average of three scans run at 50 nm/min with a 2 s response time. Thermal stabilities of constructs were evaluated by monitoring ellipticity at 208 nm. Temperature was increased at a rate of 50 °C/h. Thermal unfolding curves were fit with a two-state unfolding model as described elsewhere (*20*).

RESULTS AND DISCUSSION

Apparent Dissociation Constant (K_d^{app}) of Wild-type (A143V) Human CMV Protease. CMV protease activity is greatly increased in 30% sucrose in a manner similar to that previously observed in the presence of 20% glycerol (*13, 14*). This is due predominantly to increased dimerization as has been shown by analytical ultracentrifugation studies (*15*). The crystal structure of CMV protease (*7*−*10*) suggests that dimerization results in the stabilization of an α-helix that contributes to the formation of the active-site cavity. All our kinetic constants were measured in 30% sucrose to facilitate characterization of the dimeric form of the proteases.

The time course for approach to the monomer−dimer equilibrium of CMV protease has been reported to be very slow in 20% glycerol. Freshly diluted CMV protease, incubated at room temperature in 20% glycerol, gradually loses a portion of its activity due to slow dissociation of the dimer to monomers (*13*). We also observed a slow approach to equilibrium for 0.05 μM CMV protease in 30% sucrose when diluted from 200 μM (Figure 2). Though, the time course in 30% sucrose is slower than that reported in 20% glycerol (*13*). After allowing diluted CMV protease to equilibrate for 18 h at room temperature, the monomer−dimer K_d of CMV protease in 30% sucrose was measured as 0.42 ± 0.12 μM with a specific activity of 3.5 ± 0.3 μM min^{-1} μM^{-1} at 30 μM substrate (Figure 3A). This K_d value presumably corresponds to the true equilibrium constant and is comparable to the equilibrium $K_d = 0.55$ μM reported for CMV protease dimer in 20% glycerol (*13*).

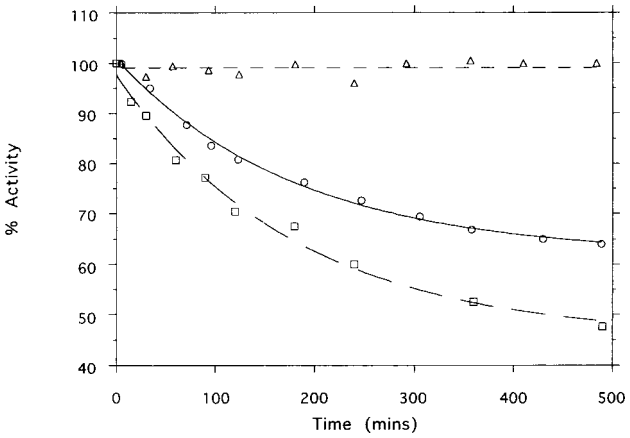

FIGURE 2: The wild-type and mutant CMV protease activity change with time; (□) wild-type, (○) R165A and (△) R166A. CMV protease wild-type (200 μM), R165A (125 μM), and R166A (150 μM) were diluted to 0.05, 0.15, and 10 μM, respectively, into a buffer containing 50 mM Hepes, 1 mM DTT, 1 mM EDTA, 150 mM NaCl, 0.01% PEG 3400, and 30% sucrose (pH 7.5 and 25 °C). After incubation time (*x*-axis) at 25 °C, aliquots were withdrawn and the activity was assayed with 30 μM substrate.

The goal of the present work has been to characterize the proteolytic kinetic properties of the dimeric form of wild-type protease and the two mutants. Our strategy was to perform measurements immediately upon dilution of the pure dimeric species into 30% sucrose assay buffer. Immediately after dilution, the proteases exhibit maximum activity which corresponds to the dimer. The extent of dimerization under these conditions was evaluated from the apparent monomer−dimer dissociation constant K_d^{app}, which was determined from the protease concentration dependence of activity (*13, 14*). For the wild-type CMV protease dimer, the observed activity at 30 μM substrate in 30% sucrose is 3.9 ± 0.1 μM min^{-1} μM^{-1} and the $K_d^{app} = 2.5 \pm 1.8$ nM (Figure 3B). This K_d^{app} value agrees with the value of 2 nM reported for the CMV protease dimer measured in the presence of 25% glycerol at pH 7.2 and 25 °C (*14*). The low K_d^{app} value indicates that, in the presence of 25% glycerol or 30% sucrose, freshly diluted CMV protease exists primarily in the dimeric form at concentrations well above 2 nM.

K_m and k_{cat} of the Wild-type (A143V) Enzyme. Although we have observed slow activity loss with time (Figure 2), presumably due to dissociation of the dimer, little (<10%) of this activity loss occurs within the first 30 min of the reaction. Thus, K_m and k_{cat} were determined within 30 min after dilution to 50 nM enzyme. In 30% sucrose, the K_m obtained was 138 ± 17 μM and the k_{cat} was 19.9 ± 1.1 min^{-1} (Table 1). These values are similar to those reported in the literature (*13, 14*) using similar peptide substrates. The K_m for the natural protein substrate is at least 46-fold lower than for our peptide substrate, but the k_{cat} is similar (*21*), suggesting that the C-terminal portion of the precursor protein contributes to substrate binding but not catalysis per se.

Enzyme Kinetics and Apparent Dimer Dissociation Constants of R165A and R166A. The K_d^{app} of R165A was also determined from the concentration dependence of activity immediately upon dilution of protease into assay buffer. As shown in Figure 4A, the K_d^{app} is 2.9 ± 0.9 nM for the R165A dimer with a specific activity of 1.6 ± 0.1 μM min^{-1}

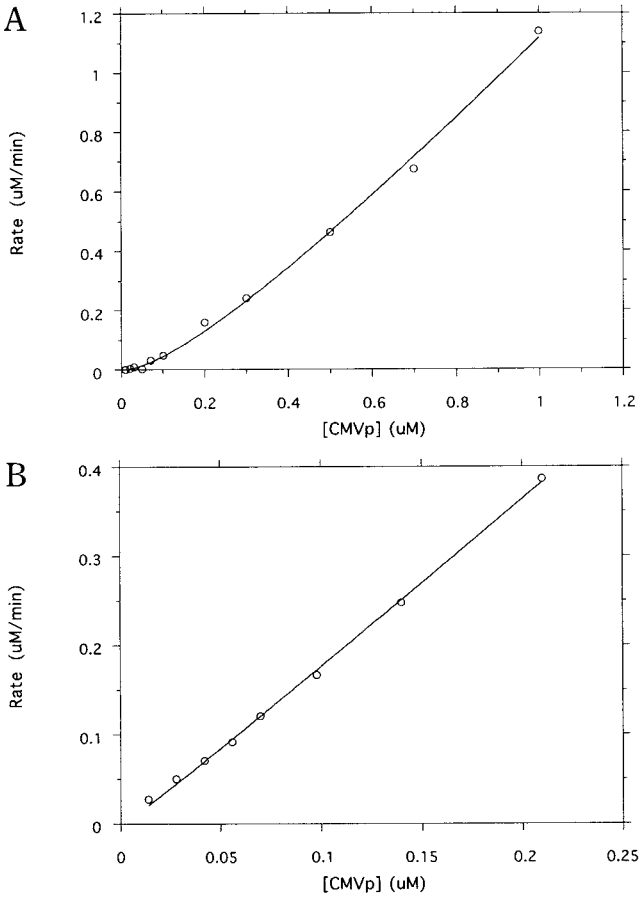

FIGURE 3: Dependence of CMV protease reaction rate on enzyme concentration, when (A) enzyme (0.01−1 μM) was assayed after 18 h incubation at 25 °C and (B) enzyme (0.01−0.2 μM) was assayed immediately after preparation from concentrated stock. The reaction was carried out in buffer containing 50 mM Hepes, 1 mM DTT, 1 mM EDTA, 150 mM NaCl, 0.01% PEG 3400, and 30% sucrose (pH 7.5 and 25 °C). Rates versus enzyme concentrations were fitted to eq 3 (see Experimental Procedures) to obtain the K_d of 0.42 ± 0.12 μM in panel A and K_d^{app} of 2.5 ± 1.8 nM in panel B.

Table 1: k_{cat} and K_m for Wild-Type, R165A, and R166A Mutant Forms of CMV Protease[a]

enzyme form	k_{cat} (min^{-1})	K_m (μM)	k_{cat}/K_m (μM^{-1} min^{-1})
wild-type[b]	19.9 ± 1.1	138 ± 17	0.14
R165A	7.4 ± 0.4	166 ± 19	0.04
R166A	0.012 ± 0.001	145 ± 18	8.3×10^{-5}

[a] Assay was carried out in the buffer containing 50 mM Hepes, 1 mM DTT, 1 mM EDTA, 150 mM NaCl, 0.01% PEG 3400, and 30% sucrose (pH 7.5 and 25 °C). [b] Wild-type means A143V mutant. In R165A and R166A, Ala 143 was also changed to Val to prevent the fragmentation of CMV protease.

μM^{-1} at 30 μM substrate in 30% sucrose. The K_d^{app} of the R165A mutant is thus essentially unchanged from that of wild-type CMV protease (2.5 ± 1.8 nM). This indicates that the Arg165 mutation of CMV protease does not effect the enzyme dimer−monomer equilibrium. The upper limit for the K_d^{app} value for the R166A mutant was determined to be 0.2 μM with a specific dimer activity of 0.003 μM min^{-1} μM^{-1} at 50 μM substrate in 30% sucrose (Figure 4B).

The K_m and k_{cat} values of the dimeric R165A mutant were determined as 166 ± 19 μM and 7.4 ± 0.4 min^{-1}, respectively. We have also observed the same time course

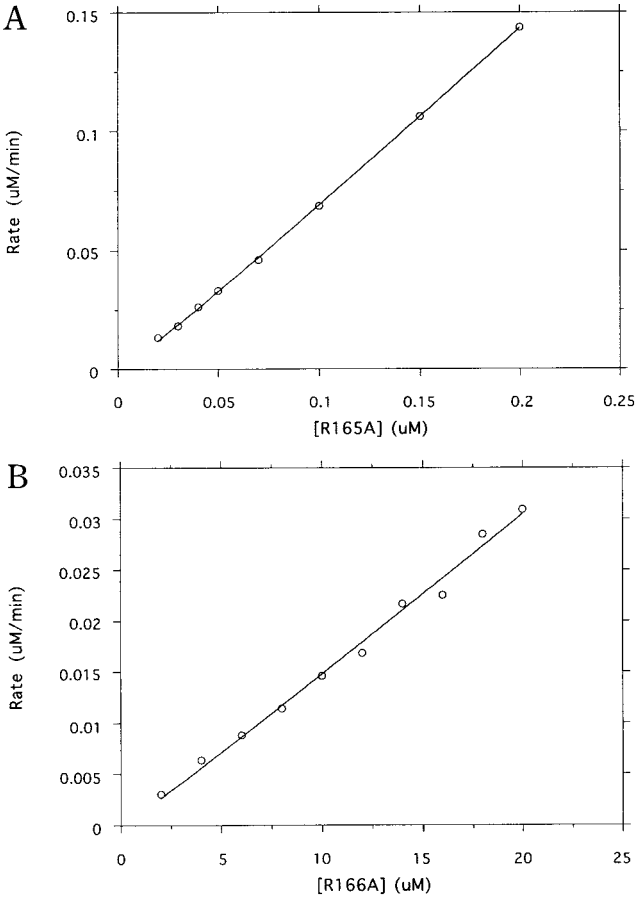

FIGURE 4: The dependence of activity of (A) the CMV protease mutant R165A and (B) R166A on enzyme concentration. The activity of enzyme was measured in buffer of 50 mM Hepes, 1 mM DTT, 1 mM EDTA, 150 mM NaCl, 0.01% PEG 3400, and 30% sucrose (pH 7.5 and 25 °C). The rates versus enzyme concentrations was fitted to eq 3 (see Experimental Procedures) to obtain the K_d^{app} of 2.9 ± 0.9 nM in panel A and upper limit K_d^{app} of 0.2 μM in panel B.

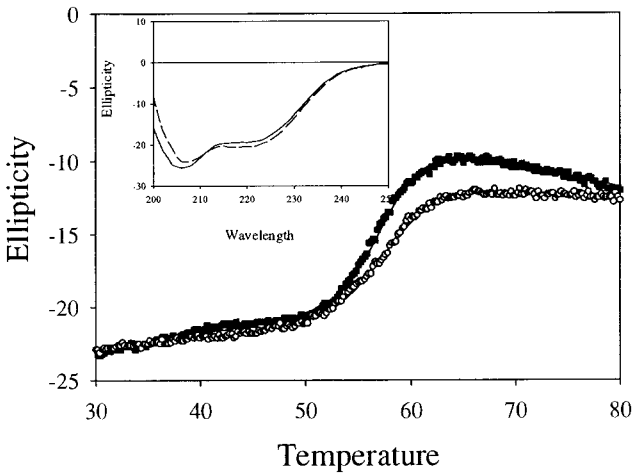

FIGURE 5: Thermal stabilities of proteases monitored by circular dichroism. Wild-type CMV protease, solid squares; R166A, open circles. Best-fit curves for fitting to a two-state unfolding model are shown along with each set of unfolding data. (Inset) Circular dichroism spectra for wild-type CMV protease (dashed curve) and mutant R166A (solid curve) at 25 °C.

of activity loss with time for 150 nM R165A incubated at 25 °C without substrate (Figure 2), and hence, measurements were conducted immediately upon dilution of the protease.

Scheme 1: The Roles of Active-Site Catalytic Amino Acids in CMV Protease Reaction

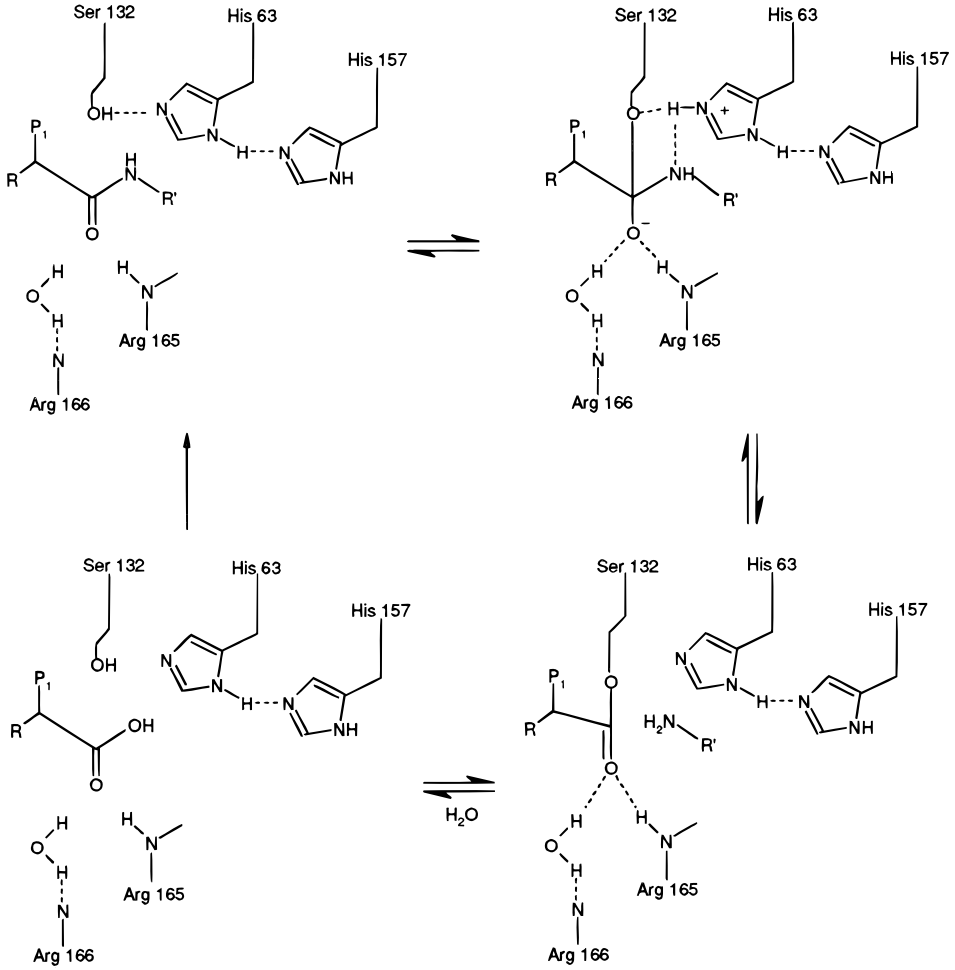

The K_m is essentially the same as that of the wild-type enzyme, while the k_{cat} is 2.7-fold reduced. The activity loss with time for 50 nM wild-type and 150 nM R165A mutant incubated at room temperature without substrate was not observed for 10 μM R166A. This is presumably due to lack of dimer dissociation at the high enzyme concentrations needed to detect activity (Figure 2). Using 10 μM enzyme, which is in large excess of its K_d^{app}, the R166A mutant was shown to have a $K_m = 145 \pm 18$ μM and a $k_{cat} = 0.012 \pm 0.001$ min^{-1}. Therefore, the R166A mutant is approximately 1700-fold less active than the wild-type enzyme.

Protein Folding of the Wild-Type CMV Protease and R166A Mutant. Because the activity of the R166A mutant was so low, we investigated whether the protease was folded properly. To do this we compared the secondary structure and thermal unfolding stabilities of wild-type and R166A mutant by circular dichroism spectroscopy. As shown in Figure 5 (inset), wild-type and R166A proteases have similar circular dichroism spectra, which indicates that the two forms are composed of the same secondary structures. The shapes of the spectra are consistent with the expected fractional contributions of α-helical and β-sheet content. The thermal stabilities of the two forms of CMV protease were also very similar (Figure 5). Half-unfolded Tms were determined from least-squares fitting as 57.4 and 57.6, respectively, for wild-type CMV and R166A protease. This indicates that their folding energies are the same and argues that the two forms share a common tertiary fold. Thus, differences in catalytic activity are most likely attributable to structural alterations restricted to the local chemical environment of the active site due to the R166A mutation.

Implications for Catalytic Mechanism. Substrate hydrolysis by classical serine proteases, esterases, and lipases occurs through a covalent tetrahedral intermediate resulting from the attack of the active-site nucleophile on the carbonyl carbon of the scissile bond. The resulting oxyanion of the substrate is stabilized through formation of strong hydrogen bonds with the amide groups of the enzyme. Unlike the classical serine proteases, the herpes proteases have a Ser-His-His catalytic triad instead of a Ser-His-Asp (*7*−*12*). This difference in the catalytic triad is believed to contribute to the large difference observed in the catalytic efficiency between the herpes proteases and classical serine proteases and to the fact that all herpes virus proteases are rather slow enzymes (*13*, *14*, *22*). For example, the catalytic efficiency of CMV protease is about 10^4 lower than that of digestive serine proteases (*23*).

There are two common models for the mechanism of serine proteases (*24*). In the "two proton transfer" model, the negatively charged aspartic acid accepts a second proton to become uncharged during the transition state. In such a model, it would be quite difficult for a histidine to play the role of the aspartic acid. In the second model, the most important role for the Asp is the ground-state stabilization of the required tautomer and rotamer of the catalytic histidine. In the crystal structures of herpesvirus protease, His63 forms

hydrogen bonds with both Ser132 and His157. A His−His interaction may have less rotameric orientations than that of His-Asp, which might be relevant to the stability of the triad in a solvent-exposed active-site cavity such as that of CMV protease (*7*). In either mechanistic model, His63 would acquire a proton in the transition state and thus become positively charged (Scheme 1). Unlike an aspartic acid, His157 will not be able to compensate for this developing positive charge but could further delocalize it. However, it is reasonable to assume that having a second histidine instead of an aspartic acid in the triad would result in a decreased catalytic efficiency owing to the weaker electronegativity of the His compared to the Asp.

On the basis of the crystal structure of CMV protease, Arg165 and Arg166 were proposed to stabilize the oxyanion intermediate formed during the reaction (*7*−*10*). Overlay of the crystal structure of CMV protease with that of trypsin reveals that Arg165 and Arg166 in CMV protease might play similar roles to Gly193 and Ser195 of trypsin. However, in trypsin, Gly193 and Ser195 provide backbone NH hydrogen bonds. In the crystal structure of CMV protease (*7*), only Arg165 backbone NH forms a hydrogen bond to the oxyanion, while Arg166 hydrogen bonds through its side chain to a water molecule which, in turn, forms a hydrogen bond to the oxyanion (Figure 1). The rationale of the stabilization of oxyanion intermediate of CMV protease is shown in Scheme 1.

CONCLUSIONS

The results presented herein are consistent with our crystallographic data (*7*, *11*, *12*), suggesting that in the herpes proteases the side chain of Arg166 (CMV protease numbering) is involved in catalysis. By replacing Arg166 of CMV protease with an alanine, it is suggested that the mutant is no longer able to hold a water molecule in the oxyanion pocket, and thus the 3 orders of magnitude reduced activity. This R166-water-oxyanion hydrogen bond thus contributes approximately 4.9 kcal/mol to the stabilization of transition state. Our data is also consistent with the absence of a role for the Arg165 side chain in catalysis. A role for Arg165 side chain in catalysis was previously suggested (*10*). Replacement of Arg165 of CMV protease by an alanine results in only 2.7-fold reduction in catalytic activity. Although our data does not directly address the suggestion that Arg165 contributes to the stabilization of the oxyanion through its backbone NH, it is nevertheless consistent with that suggestion. The R165A mutant remains active since it can stabilize the oxyanion through its Ala backbone NH. However, the 2.7-fold lower activity suggests perturbation of the environment around residue 165.

These studies are reminiscent of those previously used to probe the role of Asn155 in stabilization of the oxyanion intermediate in the bacterial serine protease subtilisin. Mutagenesis of Asn155 to Leu led to a mutant enzyme with unaltered K_m but 200−300-fold decrease in k_{cat} (*25*). The reduced enzyme activity was attributed to the inability of Leu155 to provide an amide side chain for hydrogen bonding to the oxyanion as has been proposed from crystallographic studies of subtilisin (*26*).

ACKNOWLEDGMENT

We thank Dr. Xiayang Qiu for preparing Figure 1. Many thanks to John Martin and Dr. Arun Patel for providing the peptide substrate used in the protein activity assay. We also thank Dr. David Tew and Dr. Christine Dabrowski for helpful discussions and Dean McNulty for technical assistance.

REFERENCES

1. Baum, E. Z., Bebernitz, G. A., Hulmes, J. D., Muzithras, V. P., Jones, T. R., and Gluzmann, Y. (1993) *J. Virol. 67*, 497−506.
2. Welch, A. R., Woods, A. S., McNally, L. M., Cotter, R. J., and Gibson, W. (1991) *Proc. Natl. Acad. Sci. U.S.A. 88*, 10792−10796.
3. Burck, P. J., Berg, D. H., Luk, T. P., Sassmannshausen, L. M., Wakulchik, M., and Villarreal, E. C. (1994) *J. Virol. 68*, 2937−2946.
4. O'Boyle, D. R., Wager-Smith, K., Stevens, J. T., and Weinheimer, S. P. (1995) *J. Biol. Chem. 270*, 4753−4758.
5. Holwerda, B. C., Wittwer, A. J., Duffin, K. L., Smith, C., Toth, M. J., Carr, L. S., Weigand, R. C., and Bryant, M. L. (1994) *J. Biol. Chem. 269*, 25911−25915.
6. Cox, A. G., Wakulchik, M., Sassmannshausen, L. M., Gibson, W., and Villarreal, W. C. (1995) *J. Virol. 69*. 4524−4528.
7. Qiu, Xiayang, Culp, J. S., DiLella, A. G., Hellmig, B., Hoog, S. S., Janson, C. A., Smith, W. W., and Abdel-Meguid, S. S. (1996) *Nature 383*, 275−279.
8. Tong, L., Qian, C., Massariol, M.-J., Bonneau, P. R., Cordingley, M. G., and Lagace, L., (1996) *Nature 383*, 272−275.
9. Shieh, H.-S., Kurumbail, R. G., Stevens, A. M., Stegeman, R. A., Sturman, E. J., Pak, J. Y., Wittwer, A. J., Palmier, M. O., Wiegand, R. C., Holwerda, B. C., and Stallings, W. C. (1996) *Nature 383*, 279−282.
10. Chen, P., Tsuge, H., Almassy, R. J., Gribskov. C. L., Katoh, S., Vanderpool, D. L., Margosiak, S. A., Pinko, C., Matthews, D. A., and Kan, C.-C. (1996) *Cell 86*, 835−843.
11. Qiu, X., Janson, C. A., Culp, J. S., Richardson, S. B., Debouck, C., Smith, W. W., and Abdel-Meguid, S. S. (1997) *Proc. Natl. Acad. Sci. U.S.A. 94*, 2874−2879.
12. Hoog, S. S., Smith, W. W., Qiu, X., Janson, C. A., Hellmig, B., McQueney, M. S., O'Donnell, K., O'Shannessy, D., DiLella, A. G., Debouck, C., Abdel-Meguid, S. S. (1997) *Biochemistry 36*, 14023−14029.
13. Darke, P. L., Cole, J. L., Waxman, L., Hall, D. L., Mohinder, K. S., and Kuo, L. C. (1996) *J. Biol. Chem. 271*, 7445−7449.
14. Margosiak, S. A., Vanderpool, D. L., Sisson, W., Pinko, C., and Kan, C.-C. (1996) *Biochemistry 35*, 5300−5307.
15. Cole, J. L. (1996) *Biochemistry 35*, 15601−15610.
16. Bachmann. (1972) *Bacteriol. Rev. 36*, 525 (Chart 8).
17. Laemmli, U.K. (1970) *Nature 227*, 680−685.
18. Towbin, H., Staehelin, T. and Gordon, J. (1979) *Proc. Natl. Acad. Sci. U.S.A. 6*, 4350−4354.
19. Gibson, W., Welch, A. R., and Hall, M. R. T. (1995) *Perspect. Drug Discov. Des. 2*, 413−426.
20. Eftink, M. R. (1995) *Methods Enzymol. 259*, 487−512.
21. Pinko, C., Margosiak, S. A., Vanderpool, D., Gutowski, J. C., Condon, B., and Kan, C. C. (1995) *J. Biol. Chem. 270*, 23634-23640.
22. Hall, D. L., and Darke, P. L. (1995) *J. Biol Chem. 270*, 22697−22700.
23. Babe, L. M., and Craik, C. S. (1997) *Cell 91*, 427−430.
24. Perona, J. J., and Craik, C. S. (1995) *Protein Sci. 4*, 337−360.
25. Bryan, P., Pantoliano, M. W., Quill, S. G., Hsiao, H. Y., and Poulos, T. (1986) *Proc. Natl. Acad. Sci. U.S.A. 83*, 3743−3745.
26. Robertus, J. D., Kraut, J., Alden, R. A., and Birktoft, J. J. (1972) *Biochemistry 11*, 4293−4303.

BI9726077